Dehydration-hydration reactivity of laumontite: analyses and tests for easy detection

ARTURO BRAVO[1,2], OSCAR JEREZ[1], URSULA KELM[1,*] AND MAURO POBLETE[3]

[1] *Instituto de geología Económica Aplicada (GEA), Universidad de Concepción, Concepción, Chile*
[2] *Current address: Institut für Mineralogie, Brennhausgasse, TU Bergakademie Freiberg, Freiberg, Germany*
[3] *Facultad de Ingeniería, Universidad Católica de la Santísima Concepción, Concepción, Chile*

ABSTRACT: Hydration reactions are known to affect rock or aggregate stability in construction; laumontite is not usually considered to be a 'problem-mineral' though drill cores from the very low-grade metamorphic altered andesites and volcanoclastic rocks from Central Chile showed detachments of shotcrete in a tunnel exposed to periodic water flow, with expandable clay phases presumed to be responsible for the observed failure. Abundant laumontite detected in the cores may also be responsible for the detachment, however, resulting from the structural expansion and contraction in response to hydration and drying. Clay reactivity in construction projects is often tested on site by 30 days of ethylene glycol exposure, but adequate monitoring options for laumontite are not deployed. Options for laumontite characterization involving a combination of water immersion and slaking and modified oedometer-based expansibility tests were used here to observe the response to laumontite expansion pressure. All tests were formulated considering minimal implementation efforts for building sites or the easy availability of analytical and testing facilities.

   Laumontite was identified by optical microscopy, semiquantitative X-ray diffraction, and automated mineralogical analysis. A combination of the latter two methods provided reliable information about the presence of sub-microscopic laumontite and a visual impression of the textural arrangement of the zeolite in the rock.

   A slaking test based on four cycles of immersion followed by drying and final application of weight (simulated overburden) is best suited to indirect detection and for demonstrating rock reactivity due to the presence of laumontite. Rocks with laumontite show expansion when crushed, recompacted and fitted into an oedometer, but mineralogical information is required for adequate interpretation of the results.

The hydration/dehydration of laumontite at ambient or near-ambient temperatures and the associated changes in crystal structure have been studied thoroughly since its first description by Coombs (1952). Later studies provided further crystal-structure refinements, with emphasis on water-site occupancies as a function of humidity and temperature, and also focused on low-temperature petrological modelling of zeolite-containing systems (*e.g.* Armbruster & Köhler, 1992; Artioli & Stahl, 1993; Gabuda & Kzlova, 1995; Kiseleva *et al.*, 1996; Stahl *et al.*, 1996; Fridriksson *et al.*, 2003; Kol'tsova, 2009). Neuhoff & Bird (2001) reported laumontite in equilibrium with leonhardite at 70–80%

relative humidity at 298.15 K and 1 bar; dehydrated laumontite should be considered the reaction product upon prograde formation from heulandite or stilbite in very low-grade metamorphic environments. Rashchenko *et al.* (2012) examined the hydration behaviour of single-crystal K,Na laumontite observing a continuous hydration with increase in cell volume of 1.4%. This contrasts with the dual hydration/dehydration behaviour and concomitant changes in unit-cell volume of Ca-laumontite investigated by humidity-controlled X-ray diffraction (XRD) at different temperatures (Fridriksson *et al.*, 2003). For an initial hydration step associated with the W5 site at low water pressures (0.11 and 5 mbar), a continuous unit-cell increase of 1.7% was observed, markedly along the *c* axis. An abrupt hydration/dehydration step was found for the W1 sites at 24–29 mbar and ambient temperature with inferred changes in unit-cell volume of ~2%.

The potential importance of this change in unit-cell volume becomes obvious by the widespread occurrence of laumontite, such as in vein fillings which have triggered the study of confined pressure-induced uptake of water and the shear resistance (Morrow & Byerlee, 1991), whereas the effect of laumontite on porosity and permeability in rocks affected by hydrocarbon production was modelled by White *et al.* (2004). Utada (2001*a*) reported the presence of laumontite in the upper zeolite facies rocks (Utada, 2001*a*), cement in sandstones with volcanic detritus (Iijima, 2001) and hydrothermal alteration (Utada, 2001*b*). Laumontite is often accompanied by corrensite. Examples of regional occurrence were summarized by Utada (2001*a,b*). More recent is the description by Weissenberger & Bucher (2010) of a regional occurrence of laumontite in veins linked to low-temperature metamorphism in the Swiss Alps; the widespread presence of laumontite linked to soda water-type groundwaters and its enhanced presence close to fracture zones was reported from across the Russian Federation by Koporulin (2013).

In terms of environmental and industrial applications of natural zeolites, laumontite appears to have received less attention than other zeolites such as clinoptilolite which is present in large amounts in tuff beds (Bish & Carey, 2001). The lack of attention results from the more dispersed presence of laumontite in rocks and its greater relevance as an indicator of very low-grade metamorphism or alteration rather than as an industrial mineral.

An almost complete dissociation appears to exist between the information on humidity-sensitive change of crystallographic parameters and any effect this might have on construction materials and work. The earliest description of laumontite as a "concrete poison" dates from the 1920s (Pearson and Loughlin, 1923). Although a volume change of 3–6% (Erlin & Jana, 2003) between a completely hydrated and dehydrated state for laumontite is small compared with the better known salt hydration distress, the presence of laumontite in aggregates exposed to wetting-drying cycles results in a disintegration or "crumbling" of the concrete as described by Erlin & Hime (2008). Hamada *et al.* (2005) reported the disintegration of concrete test blocks with laumontite-bearing aggregates after 27 years of exposure to a marine environment. Damage was less for tidal environments, whereas ambient exposure did not generate damage. No clear mechanism of damage could be postulated due to the experimental design. The possible mechanisms of concrete scaling were discussed in detail by Jana (2007), with air entrainment and vertical drainage as key factors to minimize scaling. The potential of laumontite crystal aggregates to disintegrate upon wetting and drying was described by Tschernich (1992) as a possible effect of cleaning laumontite micromounts.

Of particular relevance to the present study are the reports on laumontite-filled fractures in rocks from the Gotthard railroad tunnel (Bucher *et al.*, 2006) and from altered basalt of the water-transfer tunnel of the Lesotho Highland Water Project (Summer *et al.*, 2009). For the latter site, Bell & Haskins (1997) reported difficulty in predicting the expansion pressure of the laumontite-bearing basalt with maximum laumontite contents of 11% over 60 days of ethylene-glycol exposure tests. These tests are often part of contractual, agreed, on-site rock and aggregate assessment.

Laumontite is reported widely in Chile in very low-grade metamorphic andesitic rocks and hydrothermal alteration associated with some Cu (Mo) deposits (Levi *et al.*, 1989; Fuentes, 2004). Zeolite-facies altered rocks are reported from the Eocene to Miocene Coya Machali and Farellones Formations (Klohn, 1960; Charrier *et al.*, 2002) comprising andesitic lavas, rhyolites, basalts and their volcanoclastic derivates (Fig. 1). Extensive tunnelling of altered andesites is common for many large Chilean mines, but rock expansion is traditionally associated with discontinuous expansion of anhydrite or smectite-swelling.

The present study was initiated at the request of a construction company to determine the presence of expandable clay phases in drill cores taken from a tunnel exposed to periodic water flow, where shotcrete
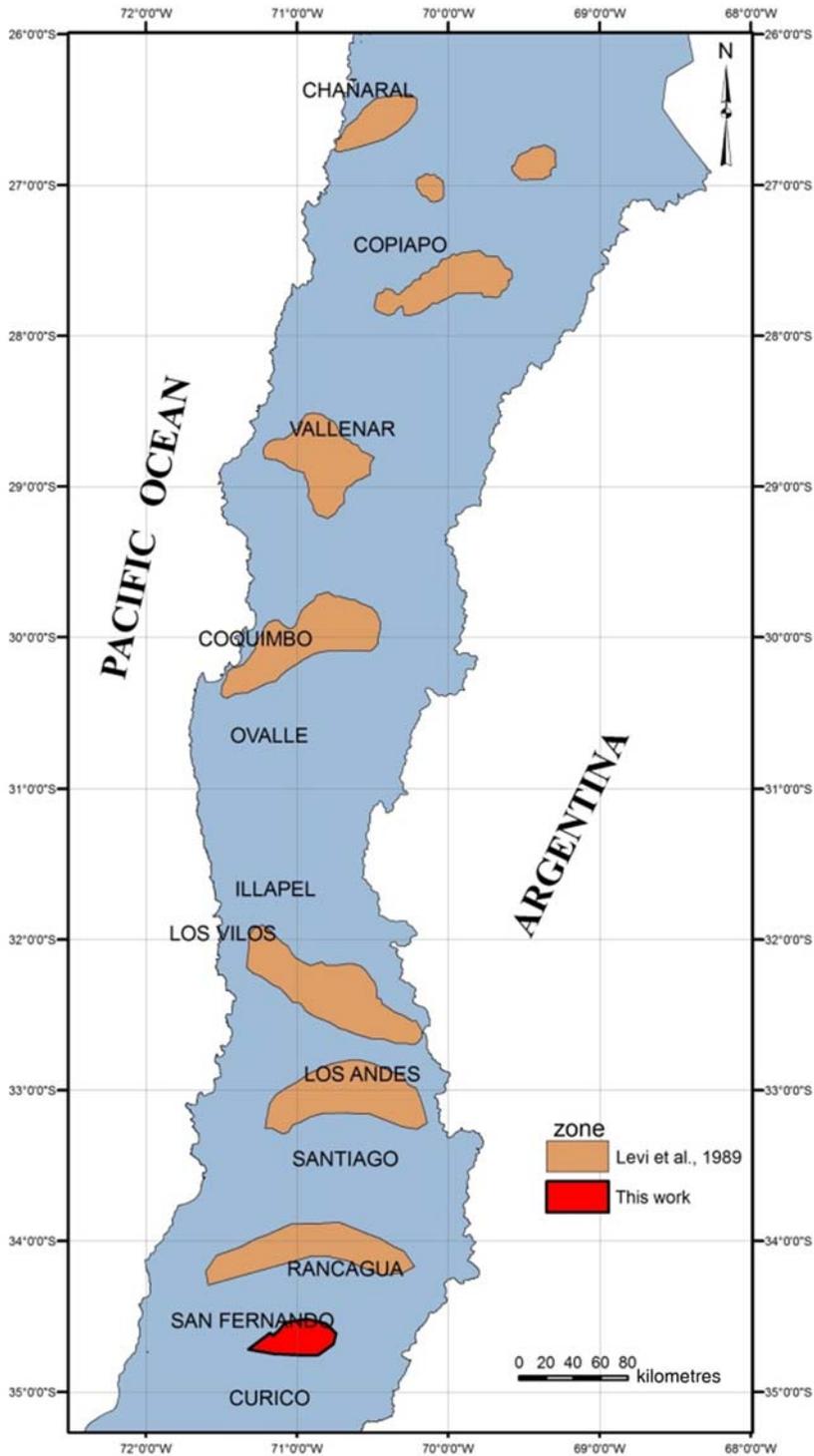
FIG. 1. Regions of Central Chile studied by Levi *et al.* (1989) where laumontite and very low-grade metamorphic mineral assemblages have been described.

failure was observed after a test phase. All contractual test work was aimed at the direct or indirect recognition of smectite, although its presence could not be inferred by ethylene glycol immersion tests carried out on site. The unexpected abundance of laumontite, with only moderate amounts of smectite required an adaptation of the rock stability tests in order to include laumontite-induced reactivity; the resulting analysis and test options are described here. In part, these tests have been adapted from hydrometallurgical extraction tests. Analytical methods and test-procedures used are those readily available and used in a mining country, but with limited requirements and tradition for mineralogical studies linked to civil engineering work.

SAMPLES AND METHODOLOGY

Analytical tools

Samples were obtained from 14 m of 10 cm-diameter diamond drill cores taken from the walls of a water-transfer tunnel in central Chile (Fig. 1). Cores were described macroscopically and divided into four groups based on colour and apparent alteration following guidelines by López (1996). Further basic characterization was by powder XRD (see below).

Uncovered thin sections were prepared, and their selection was based on the apparent alteration and/or absence of vesicles or fractures. A Nikon Optishot polarizing microscope was used. Nine of these thin sections were analyzed by Qemscan® (Quantitative Evaluation of Minerals by Scanning Electron Microscopy) using an FEI Quanta 650 microscope with backscattered electron and 2 Dual energy dispersive XFlash 6030 detectors. The purpose of this examination was the improved visualization of laumontite in false colours to detect any directionality in its distribution as well as evaluation of this method as a means of microchemical semi-quantification of laumontite abundance. In order to detect laumontite, the microchemical reference database of the automated mineral analyzer had to be adjusted somewhat in order to ensure differentiation from the compositionally similar plagioclases. Other silicate phases such as amphiboles were not specifically adjusted. Note that the spatial resolution of instruments dedicated to automated mineral analysis is subject to the pixeling of the scans and the electron optical resolution of the supporting electron microscope, with a lower limit of 2 μm for the present set up. X-ray diffraction (XRD) analyses were carried out on whole-rock powders using Bruker D4 and Rigaku Dmax-C diffractometers with a

Lynxeye and scintillation detectors, respectively; both instruments used Ni-filtered Cu-radiation. Semi-quantification was carried out using the *Autoquan* v. 2.1.6 software. No structural refinement of laumontite was carried out as this level of characterization is not likely to be needed for civil engineering works and is not a standard procedure offered by service laboratories outside of research institutions. The <2 μm fraction was separated by ultrasonic disaggregation, centrifugation and 0.45 μm porosity membrane filtration for oriented clay mounts. These were scanned at ambient humidity and saturated with ethylene glycol followed by heat treatments at 375°C and 550°C.

Prediction tests

In Chile, requests for mineralogical characterizations in civil engineering projects is unusual; this is due, in part, to a regulatory framework which does not specifically require this information. In order to predict a potential disintegration of rock due to the hydration-dehydration of laumontite, simple on-site tests were adapted from the procedure used to detect swelling pressure from expandable clays (Paige-Green, 2008; Leyland *et al.*, 2013). For these measurements, 40 pieces of 2–3 cm-sized rock chips (cleaned of any dust using pressurized air) were submerged in ethylene glycol for 30 days and any deterioration of the rock chips was monitored at regular intervals on a scale of 0–3, where 0 corresponds to unaltered and 1–3 to increasing disintegrated rock (Table 1). An average alteration index was calculated at the end of the observation. As the channel size of laumontite (4×5 Å, Armbruster & Gunter, 2001) is too small for ethylene glycol molecules, an analogue abbreviated test was carried out in water for a duration of 4 days. On the final day, a pressure of 1 kg cm^{-2} was applied to each of the rock pieces to enhance any already initiated

TABLE 1. Degrees of deterioration for each subsample. The overall deterioration is the average degree of deterioration for the rock chips used.

Level	Indicators of deterioration
0	No deterioration.
1	Minor laminar or tubular detachments from subsample surface.
2	Detachment of material, subsample disintegration into two or three parts.
3	Complete disintegration of subsample.

disintegration. The state of disintegration was registered after 1, 3, 6, 12, 48 and 96 h. The deleterious effect of laumontite in concrete aggregates becomes most obvious after wetting-drying cycles, and a slaking test was therefore introduced where 20 rock chips were exposed to four cycles of water immersion (24 h) followed by drying at 80°C (48 h), again registering the deterioration on a scale of 0–3 with a final application of 1 kg cm^{-2} pressure. The state of deterioration was registered at the end of each immersion-drying cycle.

Extended testing times (weeks) are needed for direct measurements of the expansion pressure on drill cores (results to be reported elsewhere), and the requirement of intact core pieces of at least 10–15 cm long for this test imply an indirect 'pre-selection' of core parts that better resisted the process of drilling and coring. A more readily available alternative is the use of soil oedometer measurements as indirect relative indicators of expansion pressures (Thuro, 1993; Rauch & Thuro, 2007). For this purpose, intact core sections adjacent to XRD-characterized samples were crushed and milled to <100 μm size and the powder was placed in rings of 50 mm diameter and 20 mm height and compacted with a hydraulic press at 70 MPa to obtain a density close to that of the original rock (1.9 g cm^{-3}). The compacted discs were fitted into oedometers (Humboldt and Controls) to measure the expansion pressures under saturated conditions at a maximum load of 1.5 MPa. Unlike the case for soil, an initial dry load of 1.5 MPa was applied prior to water saturation. Expansion was monitored over a span of 4 to 24 h. If no expansion occurred, the load was removed, waiting for the aforementioned time interval. If expansion occurred during any of these load steps, additional loading was halted until expansion did not increase further. Depending on the number of load steps applied, the test lasted 6–9 days. Once all load had been removed, free (non elastic) expansion was observed. The expansion pressure observed with this test is not a quantitative indicator of how much the rock will expand, due to the alteration of the original rock texture by milling and re-compaction. However, the test is sufficiently 'rapid' to obtain a qualitative demonstration of any expansion and the load at which it is observed.

RESULTS AND DISCUSSION

Lithology and mineralogy

Macroscopically, the cores consist of grey andesites with an altered groundmass (potassic alteration) and plagioclase phenocrysts up to 4 mm long. Some sections have a reddish colour which is due to finely dispersed hematite (identified in thin sections); grey-greenish hues are due to chlorite. Minor lithic tuffs are intercalated. The cores fracture along calcite-, zeolite- or quartz-filled polydirectional veins, thereby limiting their use *a priori* for direct measurements of expansion pressures (see below). Amygdales are filled with calcite and laumontite. Minor anhedral and subhedral clinopyroxene is present.

On a microscopic scale the andesite displays a porphyric texture with coarse- to medium-grained phenocrysts, a pilotaxitic fine-grained groundmass; either a subparallel orientation of the plagioclase microlites or a glomerophyric clustering is observed. Some of the andesites show evidence of auto-brecciation as described from the flanks of lava flows (Mackenzie *et al.*, 1982). Pyroclastic layers are intercalated between the andesites; here laumontite is also found in vesicles together with occasional pumpellyite.

The mineralogy (XRD) is summarized in Tables 2 and 3, which reveal that laumontite is the predominant zeolite, with minor analcime. Minor corrensite and nontronite were detected using oriented mounts of the <2 μm fraction.

The drill-core mineralogy corresponds well with observations made by Levi *et al.* (1989) and Fuentes (2004), both of which employed optical microscopy, which made the andesites of the Coya Machalí Formation text book examples of very low-grade metamorphic facies (Frey & Robinson, 1999; Robinson *et al.*, 2004).

The unequivocal identification of zeolites by optical microscopy alone is only possible for large crystals, which typically do not occur in the very low-temperature altered andesites of central Chile. In contrast, XRD analysis permits the easy identification of the zeolites, but information on any preferred orientation of laumontite is lost. As a compromise for retaining textural information, automated microchemical analysis was tested as a possible means of visualizing the distribution of laumontite to a resolution of 2 μm (Fig. 2).

Table 3 (semi-quantitative XRD and automated mineralogical analysis *via* Qemscan®) compares the semi-quantitative XRD data and the corresponding microchemistry-based mineralogy obtained by Qemscan®. For both analyses the focus was the detection/visualization of laumontite. For both methods, mineral phases exist that are not adequately analysed with routine sample-preparation procedures

TABLE 2. Mineral assemblages detected by XRD.

Minerals	M1	M2	M3	M4	M5	M6	M7	M8	M9	M10	M11	M12	M13
Albite	x	x	x	x			x	x	x	x	x	x	x
Andesine					x	x							
Laumontite	x	x		x			x	x	x	x	x	x	x
Quartz	x	x	x	x	x	x	x	x			x	x	
Chlorite	x	x	x	x	x	x	x	x	x	x	x	x	x
Hematite	x	x	x	x	x	x	x	x	x	x	x	x	x
Sanidine			x	x	x	x	x	x					
Orthoclase		x									x	x	
Calcite	x	x	x	x			x	x	x	x	x		x
Clinopyroxene		x	x	x	x	x	x	x	x				
Corrensite[a]				x	x	x	x	x	x	x			x
Nontronite[a]				x								x	x
Muscovite			x									x	x
Actinolite								x					
Analcime									x	x			

[a]Results based on oriented mounts of the <2 μm fraction.

TABLE 3. Semi-quantitative XRD and automated mineralogical analysis using Qemscan®.

Minerals	M1	M2	M3	M4	M5	M6	M7	M8	M9	M10
(a) Semi-quantitative XRD, Rietveld refinement (%)										
Plagioclase	39	33	48	47	68	64	62	42	51	45
K-Feldspar		9	3	5	13	14	2	6		
Quartz	20	22	4	4	13	13	14	9		
Laumontite	30	24	30	29				21	34	40
Hematite	4	4	9	8	2	4	5	6	9	8
Calcite	1	2	<1	<1			4	7	<1	<1
Chlorite	6	7	5	6	4	4	6	3	4	3
Smectite			2	3		1		3	3	3
Muscovite							8			
Analcime										<1
Actinolite								3		
(b) Automated mineralogical analysis, Qemscan® (%)										
Plagioclase	35.7	41.5	46.1	44.8	39.6	38.9	53.0	38.4	45.3	45.4
K-Feldspar	10.1	6.9	0.8	0.4	19.3	17.5	7.2	2.4	2.1	1.7
Quartz	22.6	17.8	3.4	2.8	12.4	11.9	11.5	4.0	0.1	0.1
Laumontite	4.7	4.6	11.3	12.7	6.0	6.0	0.1	18.3	14.2	8.0
Hematite	0.5	0.4	1.0	0.6	2.2	1.8	2.3	0.4	0.3	0.3
Calcite	0.3	0.3	0.1	0.1	0.0	0.2	0.6	1.1	0.4	0.3
Chlorite	1.3	2.3	7.7	7.7	0.9	2.4	5.1	3.2	2.9	2.8
Phyllosilicates	12.5	12.2	8.0	8.1	6.5	8.7	12.8	7.0	11.3	11.1
Epidote	0.0	0.0	0.2	0.1	0.3	0.4	0.0	0.1	0.1	0.1
Titanite	0.9	1.0	2.7	2.3	0.3	0.4	0.2	1.6	2.1	2.1
Apatite	0.2	0.2	0.0	0.0	0.4	0.4	0.3	0.0	0.0	0.0
Amphibole	4.5	5.8	9.2	10.6	6.5	5.4	0.9	13.9	13.3	17.4
Pyroxene	1.8	2.4	2.8	3.0	2.5	1.4	0.9	2.3	0.7	1.2
Fe-Ti oxides	1.1	1.0	0.9	1.1	1.3	1.5	1.9	1.7	2.1	2.4
Goethite	3.7	3.4	5.8	5.6	1.2	2.7	2.9	5.5	4.7	5.7
Others	0.2	0.2	0.2	0.4	0.4	0.5	0.3	0.3	0.5	1.5

Dehydration-hydration reactivity of laumontite
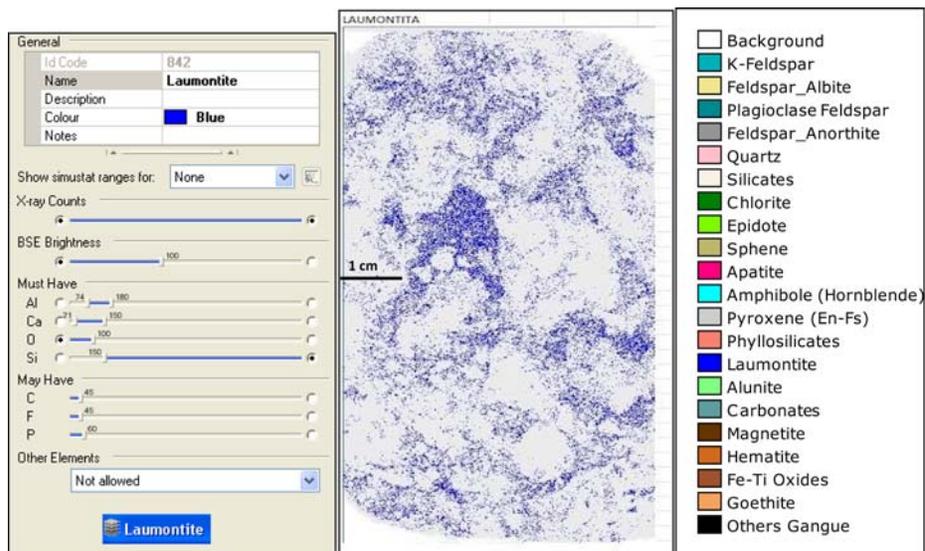
F<small>IG</small>. 2. Example of setting for the Qemscan® system and thin section with patchy, but pervasive laumontite distribution. For clarity, only laumontite is displayed.

and instrument settings, *e.g.* smectite for XRD and iron oxides for automated mineralogy. In addition to the inherent differences between these analytical methods, samples for XRD are whole-rock crushed and milled core pieces, whereas thin sections were chosen as specimens of contrasting macroscopic textures. Despite its shortcomings, this global comparison demonstrates that XRD determinations of laumontite are greater than found with Qemscan® due to the incorporation of very fine-grained zeolite, below the
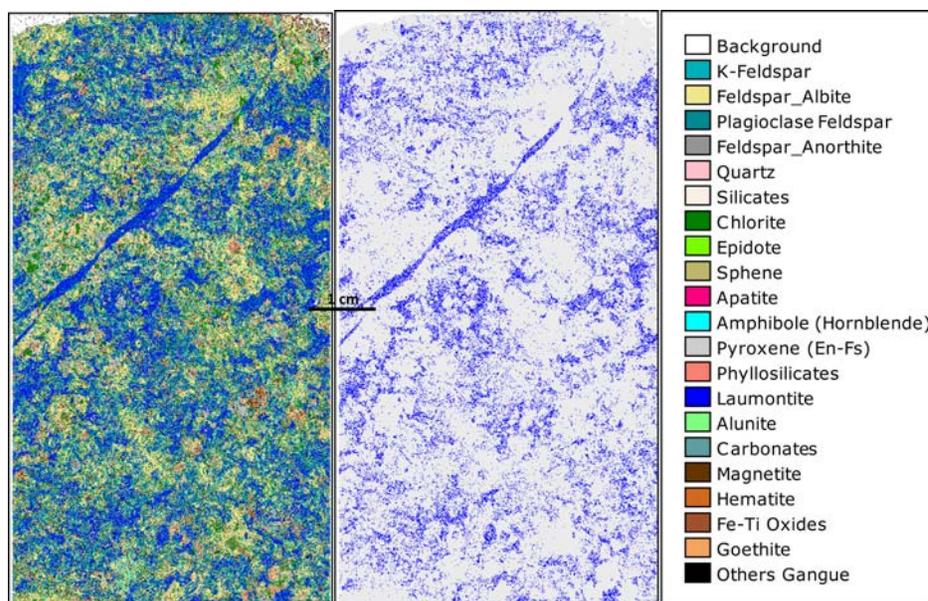
F<small>IG</small>. 3. Massive and vein-bound laumontite in sample M8, right slide displaying only laumontite.
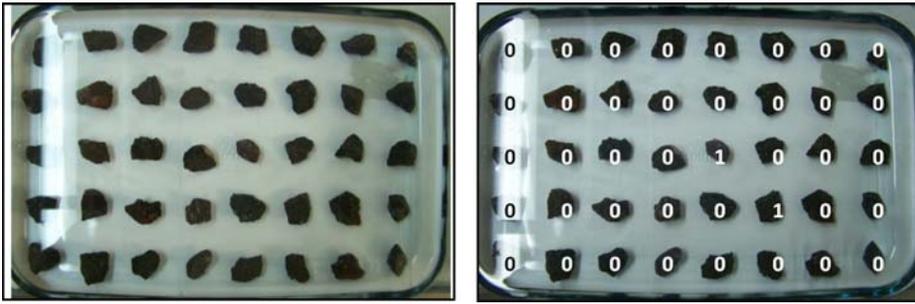
F**IG**. 4. Sample M6 at the start (left) and after 30 days of ethylene glycol submersion (right). Averaged index of deterioration = 0.05.

detection limit of electron optical resolution of the microchemical approach. Even though very fine-grained laumontite cannot be resolved by electron optical methods, it is possible to visualize clearly the pervasive and vein-bound presence of laumontite (Fig. 3) or isolated occurrences, limited, *e.g.* to amygdales, where the movement of thermal or moisture fronts within the rock had localized effects rather than affecting the overall cohesion of the rock. An amygdale-only presence of laumontite was not found for the cores studied.

Expansion tests by disintegration

As tests for the presence of smectite in soils or rock are carried out routinely on site for major building projects in Chile, options to predict in a similar way the expandability or tendency of rock disintegration due to the presence of laumontite were evaluated. Options to offer a more visual reactivity test than conclusions based on mineralogical analysis alone were also considered.

The first line of testing is a modification and abbreviation of the ethylene glycol test for assessing the durability of basic crystalline materials for rock aggregate proposed by Paige-Green (2008). This test in its original version was also applied to the cores of this study and triggered the development of the current modified tests. Submersion in ethylene glycol for 30 days did not result in partition of any of the rock pieces and only minor particle detachment was observed (level 0 or 1 damage according to test protocol) when corrensite was present (Fig. 4, Table 2). The cores studied displayed a greater laumontite content than the basaltic sequence from Lesotho (Summer *et al.*, 2009), where laumontite reached only 11 wt.% (based on XRD analysis) but also generated rock detachments in a water-transfer tunnel.

As laumontite generates scaling in response to dry-wet cycles (Jana, 2007), ethylene glycol was replaced by water using the same set-up, but with 20 rock chips of $\sim$2–3 cm size. Non-standardized tests on the resistance of crushed rock agglomerates in heap leach operations for Cu recovery consider the application of a weight (1 kg cm^{-2}) to the agglomerates at the end of their acid exposure to demonstrate, within a short test period, the comportment of the material with
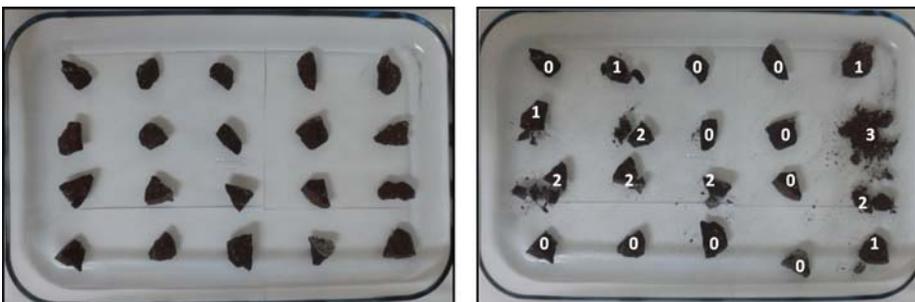
F**IG**. 5. Sample M8 in water submersion test and final pressure application, start of test (left), end of test (right). Averaged index of deterioration = 0.85.

F<small>IG</small>. 6. Sample M1 in slake test. Start of test (left), end of test (right). Averaged index of deterioration = 1.45.

overburden in analogy to overlying material in the heaps (Helle *et al.*, 2010). For the laumontite-bearing rock at each observation stage (1, 3, 6, 12, 48, 96 h) the same weight was applied to each particle in order to enhance any damage from water immersion. Again, for this case the maximum alteration level was 1 (Fig. 5).

In order to simulate the drying phase, a slaking durability test was conducted on 20 rock chips (see methodology) where a weight was applied to the rock chips only at the end of the fourth and final cycle. Here, a clear detachment of rock material was observed (Fig. 6), suggesting that simulated wetting and drying cycles are most promising in terms of identification of potential rock deterioration due to the presence of laumontite on site, with a minimal experimental set up. The massive and pervasive presence of laumontite (as shown in Fig. 3) is considered to be responsible for the partial disintegration of the rock. None of the cores tested presented laumontite in amygdales only; such an isolated zeolite occurrence will require testing by the same procedure with samples from a different site.

Oedometer expansion-tests

The second line of testing was derived from standard procedures for oedometer testing of dry and water-saturated soils (González de Vallejo *et al.*, 2002), using instead a coarsely ground rock that was re-compacted to an average density of 1.9 g cm^{-3}. This alternative approach was chosen because direct measurements of expansion pressures on cores often encounter limitations with respect to laboratory availability and corresponding long waiting times. Oedometers are more readily available to measure expansion pressure of soil. Samples selected for this test corresponded to core sections with sufficient material (1 kg) of one macroscopic rock type. Sample M7 is a fractured porphyric andesite with chlorite-corrensite alteration

(Table 2); sample M12 is an andesitic breccia with diaclases in plagioclase and fractures filled with laumontite, and sample M13 is a reddish tuff with corrensite and laumontite (Table 2). Table 4 shows the loads and corresponding expansions registered. Samples M7, M12 and M13 showed expansion, so this test is considered to be 'non-specific' with respect to the mineral causing the expansion.

Comparison of tests

The preceding mineralogical characterization and expandability tests carried out on laumontite rock suggest three possible options to evaluate potential rock reactivity due to changing moisture regimes. X-ray diffraction-based mineralogy combined with automated mineral analysis mapping of laumontite for textural assessment will allow a 'reactivity alert' based on mineralogical information alone. In addition, published local records on laumontite in low-temperature metamorphic and hydrothermal alteration mineral assemblages may provide an initial indication of the potential need for laumontite-specific testing; this simple resource is not always used due to lack of connectivity between mineralogy and geomechanical evaluation. In particular, for outcrops generated by construction works, such as tunnels, no weathered rock surfaces are available that could allow observation of the crumbled, powdery appearance of disintegrated laumontite crystal aggregates (Erlin & Hime, 2008). Clay size-fraction preparations will be necessary for the identification of minor smectite or corrensite, as has been the case for the present study. Corrensite has been reported as part of the alteration mineralogy of fossil or active geothermal fields in Chile (Vázquez *et al.*, 2014 and literature cited therein), replacing plagioclase. Corrensite is also known to occur in supergene alteration of porphyry copper deposits in the north of

TABLE 4. Direct expansion pressure test for samples M7, M12 and M13.

Sample M7		Sample M12		Sample M13	
Load (kPa)	Deformation (mm)	Load (kPa)	Deformation (mm)	Load (kPa)	Deformation (mm)
100	0.083	100	0.025	50	0.043
350	0.176	350	0.127	150	0.091
750	0.306	750	0.213	350	0.175
1,000	0.350	1,000	0.244	750	0.282
1,250	0.358	1,500	0.307	1,000	0.325
				1,500	0.401
Unloading (kPa)	Deformation (mm)	Unloading (kPa)	Deformation (mm)	Unloading (kPa)	Deformation (mm)
1,250	0.358	1,500	0.356	1500	0.440
750	0.358	750	0.338	750	0.439
350	0.322	350	0.338	350	0.439
100	0.202	100	0.280	150	0.411
0	−0.041	0	0.023	50	0.320
				0	0.150

the country, although this information is typically included in proprietary documents. The present authors found no evidence of corrensite in Chile which has been confirmed to have generated geo-mechanical problems; samples with corrensite in the present study display insignificant disintegration upon prolonged ethylene glycol immersion, leaving laumontite hydration distress as the sole cause of rock disintegration.

This mineralogical assessment alone may not be the approach taken by the construction industry, however; a slaking test parallel to the established ethylene glycol saturation test will require only minimal effort to implement on site, as well as generating the most visual results of laumontite-induced rock disintegration. Due to the potential presence of corrensite in laumontite-bearing, very low-temperature metamorphic or altered assemblages, the concomitant monitoring of rock stability under ethylene glycol exposure should be considered. As reported by Fridriksson *et al.* (2003), the discontinuous hydration at ambient temperature and medium humidity fits well with environments encountered in road or mine tunnels. Assigning rock disintegration to a particular laumontite distribution within a rock (veins and pervasive presence for the cores studied) should still be treated with caution based on the tests described, as few very low-temperature altered andesites show a single type of laumontite occurrence. Where possible, macroscopic inspection of vein patterns is recommended at the point at which

rock chips are selected for disintegration tests. Oedometer tests on crushed and re-compacted rock record expansion, although not unequivocally assigned to laumontite, should always be evaluated in combination with mineralogical information. This combination does represent a time- and cost-efficient option, in particular for rocks where cores do not fulfill the minimum dimensions of direct expansion-pressure measurements.

SUMMARY AND CONCLUSIONS

Cores from the very low-grade metamorphic altered andesites and volcanoclastic rocks of the Coya Machalí Formation in Central Chile showed detachments of shotcrete in a tunnel exposed to periodic water flow. The abundant presence of laumontite is considered to be responsible for the structural instabilities due to the expansion and contraction of the laumontite structure in response to hydration and drying. As this zeolite is widespread in very low-grade metamorphic andesitic rocks of the Andes, mineralogical analysis has been combined with water immersion, slaking and modified oedometer-expansibility tests to observe the macroscopic response to laumontite expansion pressure. All tests were set up considering minimal implementation efforts for building sites or the general availability of testing facilities.

Laumontite was identified by optical microscopy, semi-quantitative XRD, and automated mineralogical

analysis. A combination of the latter two methods is recommended to provide information on the presence of sub-microscopic laumontite as well as providing a visual impression of the textural arrangement of the zeolite in the rock.

Tests for rock stability based on ethylene-glycol exposure (Paige-Green, 2008) do not respond to the abundant presence of laumontite, nor do tests based on water immersion only. A slaking test based on four cycles of immersion followed by drying and final application of weight (simulated overburden) is most suitable to indirect detection and demonstration of rock reactivity due to laumontite. Rocks with laumontite show expansion when crushed, re-compacted and fitted to an oedometer, but mineralogical information is required to assign the reactivity to this zeolite correctly.

REFERENCES

Armbruster T. & Gunter M.E. (2001) Crystal structures of natural zeolites. Pp. 1–67 in: *Natural Zeolites. Occurences, Properties, Applications*. Reviews in Mineralogy and Geochemistry **45** (D.L. Bish & D. W. Ming, editors). Mineralogical Society of America, Chantilly, Virginia, USA.

Armbruster T. & Köhler T. (1992) Rehydration and dehydration of laumontite, a single crystal study at 100 K. *Neues Jahrbuch für Mineralogie, Monatshefte*, 385–397.

Artioli G. & Stahl K. (1993) Fully hydrated laumontite – a structure study by flat plate and capillary powder diffraction techniques. *Zeolites*, **13**, 249–255.

Bell F.G. & Haskins D. R. (1997) A geotechnical overview of Katze Dam and Transfer Tunnel, Lesotho, with a note on basalt durability. *Engineering Geology*, **46**, 175–198.

Bish D.L & Carey J.W. (2001) Thermal behavior of natural zeolites. Pp. 404–452 in: *Natural Zeolites. Occurrences, Properties, Applications*. Reviews in Mineralogy and Geochemistry, **45** (D.L. Bish & D.W. Ming, editors). Mineralogical Society of America, Geochemical Society.

Bucher K., Seelig U. & Stober I. (2006) Water in fractured crystalline rocks, data from the Gotthard railroad tunnel. *Geochimica et Cosmochimica Acta*,

Goldschmidt Conference Abstracts, A71. doi: 10.1016/j.gca.2006.06.246

Charrier R., Baeza O., Elgueta S., Flyn J., Gans P., Kay S., Muñoz N., Wyss A. & Zurita E. (2002) Evidence for Cenozoic extensional basin development and tectonic inversion south of the flat-slab segment, southern central Andes, Chile (33°–36°S.L.). *Journal of South American Earth Sciences*, **15**, 117–139.

Coombs D.S. (1952) Cell size, optical properties and chemical composition of laumontite and leonhardite. *American Mineralogist*, **37**, 812–830.

Erlin B. & Hime W. (2008) Back to the lesser known evils of the concrete world. *Concrete Construction*, **July 2008:** (Accessed September, 2016).

Erlin B. & Jana D. (2003) Forces of hydration that can cause havoc in concrete. *Concrete International*, **25**, 51–57.

Frey M. & Robinson D. (1999) *Low-Grade Metamorphism*. Blackwell Sciences, London, UK, 313 pp.

Fridriksson T., Bish D.L. & Bird D.K. (2003) Hydrogen-bonded water in laumontite I: X-ray powder diffraction study of water site occupancy and structural changes in laumontite during room-temperature isothermal hydration/dehydration. *American Mineralogist*, **88**, 277–287.

Fuentes F. (2004) *Petrología y metamorfismo de muy bajo grado de unidades volcánica oligomiocenas en la ladera occidental de los Andes de Chile Central (33° S)*. Doctoral thesis, Department of Geology, Universidad de Chile, Santiago de Chile, 398 pp.

Gabuda S.P. & Kzlova S.G. (1995) Guest-guest inter-action and phase transition in the natural zeolite laumontite. *Journal of Inclusion Phenomena and Molecular Recognition in Chemistry*, **22**, 1–13.

González de Vallejo L.I., Ferrer M., Ortuño L. & Otero C. (2002) *Ingeniería Geológica*. Pearson, Prentice Hall, Madrid, 715 pp.

Hamada H., Yamaji T., Mohammed T.U. & Torii K. (2005) Unexpected expansion of concrete with laumontite containing aggregates under seawater conditions. *Asian Journal of Civil Engineering (Building and Housing)*, **6**, 361–372.

Helle S., Jerez O., Kelm U., Pincheira M. & Varela B. (2010) The influence of rock characteristics on the acid leach extraction and re-extraction of Cu-oxide and sulfide minerals. *Minerals Engineering*, **23**, 45–50.

Iijima A. (2001) Zeolites in petroleum and natural gas reservoirs. Pp. 347–402 in: *Natural Zeolites. Occurrences, Properties, Applications*. Reviews in Mineralogy and Geochemistry **45** (D.L. Bish & D.W. Ming, editors). Mineralogical Society of America, Chantilly, Virginia, USA.

Jana D. (2007) Concrete scaling – a critical review. *Proceedings of the twenty-ninth conference on cement microscopy*, Quebec, Canada, May 20–24th.

Kiseleva I., Navrotsky A., Belitsky I.A. & Fursenko B.A. (1996) Thermochemistry of natural potassium sodium

calcium leonhardite and its cation-exchange forces. *American Mineralogist*, **81**, 668–675.

Klohn E. (1960) *Geología de Santiago, O'Higgins, Colchagua y Curicó*. Instituto de Investigaciones Geológicas, Santiago de Chile, Boletín, **8**, 95 pp.

Kol'tsova T.N. (2009) Crystal structures of CaO-Al$_2$O$_3$-SiO$_2$-H$_2$O-Zeolites. *Inorganic Materials*, **45**, 99–115.

Koporulin V.I. (2013) Formation of laumontite in sedimentary rocks: A case study of sedimentary sequences in Russia. *Lithology and Mineral Resources*, **48**, 122–137.

Levi B., Aguirre L., Nyström J. O., Padilla H. & Vergara M. (1989) Low-grade regional metamorphism in the Mesozoic-Cenozoic volcanic sequence of the Central Andes. *Journal of Metamorphic Geology*, **7**, 487–495.

Leyland R.C., Paige-Green P. & Momayez M. (2013) Development of the road aggregate specification for the modified ethylene glycol durability index for basic crystalline material. *Journal of Materials in Civil Engineering*, doi: 10.1061(ACSE)MT.1943-5533.0000946.

López C. editor (1996) *Manual de rocas ornamentales. Prospección, explotación, elaboración y colocación*. Entorno Gráfico, Madrid, 696 pp.

Mackenzie W.S., Donaldson C.H. & Guilford C. (1982) *Atlas of Igneous Rocks and Their Textures*. Halstead Press, New South Wales, Australia, 148 pp.

Morrow C.A. & Byerlee J.D. (1991) A note on the frictional strength of laumontite from Cajon pass, California. *Geophysical Research Letters*, **18**, 211–214.

Neuhoff P.S. & Bird D.K. (2001) Partial dehydration of laumontite: thermodynamic constraints and petrogenetic implications. *Mineralogical Magazine*, **65**, 59–70.

Paige-Green P. (2008) A revised ethylene glycol test for assessing the durability of basic crystalline materials for rock aggregate. *International Geological Congress*, Oslo, Norway, August 6–14th, MRC-08 Geological Construction Materials, Part 1, accessed through: www.cprm.gov.br/33IGC/1323199.html (accessed September 2016).

Pearson J.C. & Loughlin G.F. (1923) An interesting case of dangerous aggregate. *Proceedings of the American Concrete Institute*, **19**, 142–154.

Rashchenko S.V., Sertyotkin Y.V. & Bakakin V.V. (2012) A X-ray single crystal study of alkaline cations influence on laumontite hydration ability: 1. Humidity-induced hydration of Na,K-rich laumontite. *Microporous and Mesoporous Materials*, **151**, 93–98.

Rauch F. & Thuro K. (2007) Rasche und optimierte Vorhersage von Quelleigenschaften bei Tonen mithilfe des Pulverquellversuches. *Veröffentlichungen von der 16. Jahrestagung für Ingenieurgeologie*, March 7th–10th, Bochum, Germany.

Robinson D., Bevins R.E., Aguirre L. & Vergara M. (2004) A reappraisal of episodic burial metamorphism in the Andes of central Chile. *Contributions to Mineralogy and Petrology*, **146**, 513–528.

Stahl K., Artioli G. & Hansen J.C. (1996) The dehydration process in the zeolite laumontite. A real time synchrotron X-ray powder diffraction study. *Physics and Chemistry of Minerals*, **23**, 328–336.

Summer P.D., Hall K.J., van Rooy J.L. & Meiklejohn K.I. (2009) Rock weathering on the eastern mountains of Southern Africa. Review and insights from case studies. *Journal of African Earth Sciences*, **55**, 236–244.

Thuro K. (1993) Der Pulverquellversuch – ein neuer Quellhebungsversuch. *Geotechnik*, **16**, 101–106.

Tschernich R.W. (1992) *Zeolites of the World*. Geoscience Press Inc., Phoenix, Arizona, USA, 563 pp.

Utada M. (2001*a*) Zeolites in burial diagenesis and low-grade metamorphic rocks. Pp. 277–304 in: *Natural Zeolites. Occurences, Properties, Applications*. Reviews in Mineralogy and Geochemistry 45 (D.L. Bish & D.W. Ming, editors). Mineralogical Society of America, Chantilly, Virginia, USA.

Utada M. (2001*b*) Zeolites in hydrothermally altered rocks. Pp. 306–322 in: *Natural Zeolites. Occurences, Properties, Applications*. Reviews in Mineralogy and Geochemistry 45 (D.L. Bish & D.W. Ming, editors). Mineralogical Society of America, Chantilly, Virginia, USA.

Vázquez M., Nieto F., Morata D., Droguett B., Carillo-Rosua F. J. & Morales S. (2014) Evolution of clay mineral assemblages in the Tinqueririca geothermal field, Andean cordillera of central Chile: an XRD and HRTEM-AEM study. *Journal of Volcanology and Geothermal Research*, **282**, 43–59.

Weissenberger T. & Bucher K. (2010) Zeolites in fissures of granites and gneiss of the Central Alps. *Journal of Metamorphic Geology*, **28**, 825–847.

White C.L.I.M., Rabdel Ruiz-Salvador A. & Lewis D.H. (2004) Pressure-induced hydration effects in the zeolite laumontite. *Angewandte Chemie, International Edition*, **43**, 469–472.